HHS Public Access

Author manuscript

Neuroimage. Author manuscript; available in PMC 2021 March 01.

Published in final edited form as:

Neuroimage. 2020 March ; 208: 116469. doi:10.1016/j.neuroimage.2019.116469.

Parasympathetic arousal-related cortical activity is associated with attention during cognitive task performance

Anita D. Barber[a,b,c,*], **Majnu John**[a,d], **Pamela DeRosse**[a,b,c], **Michael L. Birnbaum**[a,b,c], **Todd Lencz**[a,b,c], **Anil K. Malhotra**[a,b,c]

[a]Department of Psychiatry, Zucker Hillside Hospital, 75-59 263rd Street, Glen Oaks, NY, 11004, USA

[b]Center for Psychiatric Neuroscience, Feinstein Institute for Medical Research, 350 Community Drive, Manhasset, NY, 11030, USA

[c]Department of Psychiatry, Zucker School of Medicine at Hofstra/Northwell, 500 Hofstra University, Hempstead, NY, 11549, USA

[d]Department of Mathematics, Hofstra University, 100 Hofstra University, Hempstead, NY, 11549, USA

Abstract

Parasympathetic arousal is associated with states of heightened attention and well-being. Arousal may affect widespread cortical and subcortical systems across the brain, however, little is known about its influence on cognitive task processing and performance. In the current study, healthy adult participants (n = 20) underwent multi-band echo-planar imaging (TR = 0.72 s) with simultaneous pulse oximetry recordings during performance of the Multi Source Interference Task (MSIT), the Oddball Task (OBT), and during rest. Processing speed on both tasks was robustly related to heart rate (HR). Participants with slower HR responded faster on both the MSIT (33% variance explained) and the OBT (25% variance explained). Within all participants, trial-to-trial fluctuations in processing speed were robustly related to the heartbeat-stimulus interval, a metric that is dependent both on the concurrent HR and the stimulus timing with respect to the heartbeat. Models examining the cardiac-BOLD response revealed that a distributed set of regions showed arousal-related activity that was distinct for different task conditions. Across these cortical regions, activity increased with slower HR. Arousal-related activity was distinct from task-evoked activity

*Corresponding author. Division of Psychiatry Research, The Zucker Hillside Hospital, 75-59 263rd Street, Glen Oaks, NY, 11004, USA. abarber@northwell.edu (A.D. Barber).

Author Credit Statement

Anita D. Barber: Conceptualization, Methodology, Software, Formal Analysis, Investigation, Data Curation, Writing – Original Draft, Writing – Review & Editing, Visualization, Project Administration; **Majnu John:** Methodology, Validation, Formal Analysis; **Pamela DeRosse:** Writing – Review & Editing, Project Administration; **Michael L. Birnbaum:** Project Administration; **Todd Lencz:** Writing – Review & Editing, **Anil K. Malhotra:** Funding acquisition, Resources, Project Administration, Supervision, Writing – Review & Editing.

Declaration of competing interest

Dr. Malhotra has served as a consultant for Forum Pharmaceuticals and has served on a scientific advisory board for Genomind, Inc. Dr. Lencz has served as a consultant to Genomind, Inc. The other authors report no financial relationships with commercial interests.

Appendix A. Supplementary data

Supplementary data to this article can be found online at https://doi.org/10.1016/j.neuroimage.2019.116469.

and it was robust to the inclusion of additional physiological nuisance regressors into the models. For the MSIT, such arousal-related activity occurred across visual and dorsal attention network regions. For the OBT, this activity occurred within fronto-parietal regions. For rest, arousal-related activity also occurred, but was confined to visual regions. The pulvinar nucleus of the thalamus showed arousal-related activity during all three task conditions. Widespread cortical activity, associated with increased parasympathetic arousal, may be propagated by thalamic circuits and contributes to improved attention. This activity is distinct from task-evoked activity, but affects cognitive performance and therefore should be incorporated into neurobiological models of cognition and clinical disorders.

Keywords

Autonomic arousal; Attention; Alertness; Processing speed; Reaction times; Thalamocortical

1. Introduction

The primary function of the autonomic nervous system (ANS) is to regulate homeostatic processes involved in arousal states. While this is integral to the maintenance of bodily functions, the ANS also plays a role in attention, cognitive processes, and mental health (Hansen et al., 2003; Porges, 2003, 2009; Thayer and Siegle, 2002; Thayer et al., 2010). Recent research suggests that on-going fluctuations in alertness activate ascending subcortical pathways that send widespread projections to the cortex thereby leading to global cortical activation (Falahpour et al., 2018; Liu et al., 2018; Turchi et al., 2018). While such fluctuating arousal evokes global cortical activity during rest, it is unknown whether such activity also occurs during cognitive task performance and whether it affects behavior. During states of low alertness, such as fatigue or sleep deprivation, cognitive performance and sustained attention are impaired (Chee and Chuah, 2008; Chee et al., 2008; Wang et al., 2016). Under usual conditions of rested wakefulness, momentary fluctuations in autonomic arousal might likewise give rise to widespread cortical activation contributing to fluctuations in task-performance. It is unknown, however, whether this is actually the case. The current study examined whether arousal-related cortical activation, reflecting the widespread influence of ascending subcortical projections, occurs during cognitive task performance and whether such arousal-related cortical activation is behaviorally-relevant.

While autonomic activity is important for cognitive function, the overwhelming majority of functional imaging studies treat physiological fluctuations (i.e. cardiac and respiratory activity) as nuisance confounds that obscure neuronal signal (Ciric et al., 2017; Power et al., 2017). Physiological activity produces periodic pulsation of the brain, which causes micro-movement artifact. A number of methods have been proposed to remove such physiological nuisance from resting-state fMRI data (Burgess et al., 2016; Chang et al., 2009; Chang and Glover, 2009; Glover et al., 2000; Muschelli et al., 2014) and recent studies likewise find that such methods improve signal in task fMRI data (Eklund et al., 2018). While physiological nuisance regression is undeniably a critical fMRI preprocessing step, there is evidence that autonomic arousal state impacts brain function and cognitive performance. Physiological noise occurs at higher frequencies (i.e. in the range of the heart rate and

respiratory rate); however, it has been noted that physiological time-courses also contain low-frequency components characteristic of neuronal activity (Bianciardi et al., 2009; Shmueli et al., 2007). The finding that fluctuations in alertness during rest reflect the influence of ascending subcortical projections on widespread cortical activation (Falahpour et al., 2018; Liu et al., 2018) supports the notion that low-frequency physiological activity is, at least partly, due to neuronal activity.

Two opposing autonomic brainstem pathways influence cortical arousal, one of which is activated by parasympathetic arterial baroreceptor activity, and the other of which is suppressed by such activity (Silvani et al., 2015). Functional imaging studies have identified patterns of brain activity which may be attributable to sympathetic and/or parasympathetic mechanisms (Beissner et al., 2013; Chang et al., 2013; Fan et al., 2012). However, a challenge in examining autonomic arousal-related cortical activity is that it is difficult to disentangle ascending and descending influences (Shoemaker et al., 2015). Many studies use cardiovascular and/or cognitive challenges to elicit cardiac changes, in which cortical activity exerts a top-down, descending influence on autonomic arousal. Cortical regions commonly considered to form the Autonomic Network (AN), such as the anterior and posterior insula, Medial Prefrontal Cortex (MPFC), SomatoMotor Cortex (SMC), Anterior Cingulate Cortex (ACC), and amygdala (Critchley, 2009; Shoemaker et al., 2015), are regions that may override the cardiac baroreflex (Shoemaker et al., 2015). Therefore, cortical activity reflecting descending autonomic pathways are evoked by task events; whereas, activity reflecting ascending autonomic pathways, in which cortical arousal results from on-going activity in autonomic brainstem nuclei, are evoked on each heartbeat (HB) by on-going cardiac baroreceptor activity. The current study, therefore, utilizes Heart Rate (HR), a direct indicator of baroreceptor activity as a means to gauge brain activity reflecting ascending autonomic arousal during both cognitive task performance and rest.

Decades of evidence relate cardiac indicators of autonomic arousal to cognitive states. Numerous studies have found that processing speed is dependent on the timing of the stimulus with respect to the cardiac cycle (Birren et al., 1963; Edwards et al., 2007; McIntyre et al., 2008; Saari and Pappas, 1976; van der Molen et al., 1983). Reaction times (RTs) tend to be faster when stimuli are presented later in the cardiac cycle. Recent studies have exploited this relationship by manipulating whether the stimulus is presented during systole or diastole (Garfinkel et al., 2013; Sandman, 1984), with some studies finding that attention is improved when stimuli are presented at diastole, but others finding that different types of attention are optimized during the two heart periods (Pramme et al., 2016). Theories that relate autonomic arousal to cognition (Porges, 2003, 2007; Thayer et al., 2009) have suggested that parasympathetic arousal, which is characterized by slower HR and greater High Frequency-Heart Rate Variability, facilitates attention and optimal mental health. While states of high parasympathetic arousal are commonly considered beneficial to cognition (Hansen et al., 2003; Porges, 1995; Porges et al., 1994; Suess et al., 1994; Thayer and Siegle, 2002), the effects that fluctuations in parasympathetic arousal have on brain function are not well understood.

Autonomic arousal may influence widespread cortical activity via ascending subcortical projections which arise from autonomic brainstem nuclei, through the Ascending Reticular

Activating System (ARAS) (Edlow et al., 2012; Yeo et al., 2013). The basal forebrain, a region that receives autonomic inputs and projects extensively to cortex has been linked to autonomic arousal (Berntson et al., 2003; Saper, 2002; Zaborszky et al., 2008). The thalamus is likewise an intermediary throughway for ascending autonomic projections, and plays a well-known role in coordinating oscillatory activity across cortical regions (Edlow et al., 2012). Numerous recent studies highlight the critical role of thalamic amplification of cortico-cortical communication in both sustained and selective attention (Crick, 1984; Nakajima and Halassa, 2017; Saalmann et al., 2012; Schmitt et al., 2017). Therefore, autonomic-related widespread cortical activation may arise from ascending autonomic projections in the basal forebrain and/or thalamus, which coordinate attention during task performance.

The current study examined autonomic-related cortical activation during task fMRI to determine whether it influences cognitive performance and whether it is task-specific. HR was monitored during resting-state as well as during performance of two tasks: the Multi-Source Interference Task (MSIT) and the Oddball Task (OBT). The use of Multi-Band Echo-Planar Imaging (MB-EPI) provided high temporal (TR = 0.72 s) resolution and allowed for a more accurate examination of cardiac-BOLD activity during task performance. The influence of autonomic arousal on brain activity was examined by convolving HR with the hemodynamic response function. This cardiac-BOLD regressor modeled brain activity that increases or decreases along with autonomic arousal. It was expected that during rested wakefulness, momentary fluctuations in autonomic arousal give rise to widespread cortical activation as well as activation within the basal forebrain and/or thalamus. Further, it was expected that such autonomic-related cortical activation will occur, not only during rest, but also during cognitive performance. Such autonomic-related cortical activity was examined during two different cognitive tasks to determine whether such activity is tailored to particular task demands.

2. Materials and methods

2.1. Participants

Twenty-one healthy adults participated in the study (60% female, mean age = 28.05 (4.29) years). Nineteen of the subjects completed all three of the task conditions within the imaging session. One participant completed only the MSIT and one participant completed the OBT and resting-state runs, but not the MSIT. Participants provided written consent upon reading a description of the study details. The study protocol was approved by the Institutional Review Board of Northwell Health.

2.2. Imaging scan acquisition

Images were acquired on a Siemens Prisma 3-T scanner at the North Shore University Hospital. All participants completed a T1-weighted scan (TR = 2400 msec, TE = 2.22 msec, voxel size = 0.8 mm^3, scan length = 6 min, 38 s) and several simultaneous MB-EPI scans (multiband acceleration factor = 8, TR = 720 msec, TE = 33.00 msec, voxel size = 2.2 × 2.2 × 2.0 mm) (Van Essen et al., 2013). The latter consisted of two resting-state runs (7 min, 17 s per run) and four runs of each of the two tasks (4 min and 2 s for each of the MSIT runs

and 2 min and 45 s for each of the OBT runs). Every other functional run was acquired in the anterior-posterior or posterior-anterior phase-encoding direction. Run order was counterbalanced between subjects. The first 13 vol of each functional run were discarded acquisitions.

2.3. fMRI tasks

2.3.1. Multi-Source Interference Task (MSIT)—All participants performed two brief practice runs before entering the scanner and four experimental runs of the MSIT while in the scanner. On each trial, three numbers appeared. Participants were instructed to respond to the number that was different from the other two and to ignore the position in which the numbers appeared. Right-hand index, middle, or ring finger responses were made to a correct answer of 1, 2, or 3, respectively. On congruent trials, the target number appeared with two neutral digits (i.e. zeros) and the position of the target digit was congruent with the correct response (i.e. 100, 020, or 003). On interference trials, the target number appeared with two interfering digits and the position of the target digit was incongruent with the correct response (e.g. 313, 112, 322).

On each trial, the stimulus appeared for 1750 msec, followed by a fixation dot for a variable jitter duration of 0–1250 msec. If a participant made an incorrect response or if they took more than the allotted 1750 ms to respond, a feedback slide stating “Incorrect” or “Too Slow” appeared in red font for 500 msec. If the participant made the correct response, the stimulus was replaced by a fixation dot for the remainder of the 1750 msec plus the jitter duration.

Each run consisted of 76 MSIT trials and started and ended with a 10 s rest period in which a fixation dot remained at the center of the screen. Three additional 10 s rest periods were included throughout the run. The first two participants performed four runs in which 50% of trials were congruent and 50% were interference trials. The remaining 18 participants performed alternating runs which consisted of a 75%:25% or 25%:75% ratio of congruent:interference trials.

2.3.2. Oddball Task (OBT)—All participants performed one brief practice run before entering the scanner and four experimental runs of the OBT while in the scanner. On each trial, a standard “O” or an oddball “X” stimulus appeared. Participants were instructed to respond with the index finger of their right hand when an “O” appeared and the middle finger of their right hand when an “X” appeared.

On each trial, the stimulus appeared for 1000 msec, followed by a fixation dot for a variable jitter duration of 0–750 msec. If a participant made an incorrect response or if they took more than the allotted 1000 ms to respond, a feedback slide stating “Incorrect” or “Too Slow” appeared in red font for 500 msec. If the participant made the correct response, the stimulus was replaced by a fixation dot for the remainder of the 1000 msec plus the jitter duration.

Each run consisted of 76 OBT trials and started and ended with a 10 s rest period in which a fixation dot remained at the center of the screen. Three additional 10 s rest periods were

included throughout the run. To establish a prepotency for standard “O” stimuli, the first three trials of each run and the first trial following a rest period were standard trials. Oddball “X” stimuli occurred on approximately 23% of trials.

2.4. Physiological measurements

During scan acquisition, a pulse oximeter recorded blood oxygen saturation through a wireless finger clip attached to the participants’ left index finger. Measurements were sampled every 4.99 ms. In order to compare HR measurements between task and rest, physiological recordings were taken during each task fMRI run (4 min, 2 s long for the MSIT and 2 min 45 s long for the OBT) as well as during each resting-state fMRI run (7 min, 17 s long).

2.5. Data analysis

2.5.1. Physiological measurement analysis

Pulse oximetry HR recordings were processed using Matlab2015b. Heartbeats (HBs) were extracted using the *peakfinder* function. Each Inter-Beat Interval (IBI) was converted to seconds. It should be noted that HR in the current study was represented as the IBI, rather than beats per minute, and therefore, faster HR is represented by smaller values (i.e. shorter IBI) and slower HR is represented by larger values (i.e. longer IBI). To ensure that HBs were not missed due to motion, any IBI greater than 2 s, or more than 4 standard deviations from the mean, was interpolated as the average of surrounding IBIs. Block HR was computed as the average IBI for each of the resting-state, MSIT, and OBT runs.

To align with task events, the time in seconds from run start was computed for the peak of each HB. Concurrent trial IBI was computed as the IBI for the nearest HB occurring after the stimulus onset (Fig. 1A). IBI was also computed for one HB occurring before and two HBs occurring after the concurrent HB (i.e. the pre-trial and two post-trial HBs). To determine whether HR was affected by the task design, linear mixed models were created for the MSIT and OBT. These examined the effects of condition (congruent/interference for MSIT or standard/oddball for OBT) and stimulus HB (sHB: before, concurrent, first after, or second after) on HR. Both subject and sHB were treated as random factors.

Associations between task performance and cardiac metrics were examined both between- and within-subjects. To determine whether HR itself, or the timing between cardiac events and task events, affected task performance, the HB-Stimulus Interval (HSI), a measure of the time between the HB before (i.e. the start of the concurrent IBI) and the stimulus onset (Fig. 1A), was examined in addition to HR. For between-subject associations between cardiac metrics (HR and HSI) and task performance (RT), the mean across all correct trials was computed for each subject. Linear regression was then used to test the cardiac-performance relationships. For within-subject cardiac-performance relationships, trials were first categorized by the post-stimulus HB in which the response occurred (i.e. rHB0, rHB1, or rHB2: Fig. 1B). This was done because, by definition, responses that corresponded to later HBs tended to be slower (i.e. mean rHB0 RT < mean rHB1 RT < mean rHB2 RT). Analyses examining the within-subjects relationship between cardiac indicators and performance were performed using four separate models, testing the effect of RT-HR and RT-HSI relationships

for both the MSIT and OBT. These linear mixed-effects models were performed using the *lme* function from the *R* package *nlme* and included subject as a random factor and condition, post-stimulus rHB (rHB0, rHB1, or rHB2), and continuous trial-level cardiac metrics (either HR or HSI) as fixed factors to predict trial-level RTs across all subjects.

2.5.2. fMRI task preprocessing and analysis—Image processing was performed using SPM12 and Matlab2015b. This included motion correction, co-registration, segmentation, normalization, and 8-mm full-width-at-half-maximum spatial smoothing. First-level general linear models (GLMs) included task condition regressors (congruent and interference for MSIT or standard and oddball for OBT) and error regressors for each run. Each of these task regressors consisted of zero-duration impulse functions that were convolved with the canonical hemodynamic response function. For each condition, additional RT regressors were created in which the height of the regressor was parametrically-modulated by the RT on each trial. Cardiac regressors assessing the impact of HR on brain activity were included. The cardiac regressors were created by placing a zero-duration impulse function at the onset of each HB and then parametrically-modulating the height of the impulse function for each HB by the length of the IBI. In SPM, creating a parametric modulation regressor results in two regressors: the unmodulated regressor, in which the impulse function amplitude is the same for each event, and the modulated regressor, in which the impulse function amplitude is a function of the modulation variable (in this case, the inter-beat interval). These two cardiac regressors were then convolved with the hemodynamic response function. We refer to the unmodulated cardiac regressor as the HB-evoked regressor and the HR-modulated regressor as the cardiac-BOLD regressor. See Figs. S1 and S2 for example cardiac-BOLD regressors and task regressors for two subjects. Additionally, a number of nuisance regressors of no interest were included. These consisted of 12 motion parameters (6 absolute and 6 differential motion regressors) and several CompCor physiological noise regressors explaining 30% of the variance in white matter and cerebrospinal fluid voxels (Behzadi et al., 2007; Muschelli et al., 2014), separately. See Fig. S3 for an example of the full design matrices for one subject's GLMs for each task. To assess potential overlap between cardiac-BOLD activity and the physiological nuisance (i.e. CompCor) regressors, follow-up GLMs were run, which excluded the CompCor nuisance regressors.

Within each subject, contrasts were created for the following effects of interest across the four runs of each task: HB-evoked, cardiac-BOLD, task-evoked activity common to both conditions (i.e. congruent + interference for MSIT and standard + oddball for OBT), task-evoked activity distinct for each condition (i.e. interference-congruent for MSIT and oddball-standard for OBT), as well as task-evoked RT regressors (i.e. congruentRT + interferenceRT for MSIT and standardRT + oddballRT for OBT). For each contrast, subject-level contrast maps were created which represent the contrast-weighted beta maps. The subject-level contrast maps were then entered into group-level one-sample t-tests to determine those voxels in which activity was significantly greater or less than zero. Significant findings were thresholded at a voxel-level of $p < 0.001$ and a cluster-level of $p < 0.001$, according to Random Field Theory (Worsley et al., 1998, 2004).

2.5.3. Follow-up examination of cardiac-BOLD in subcortical regions—Due to low signal-to-noise ratio (SNR) in subcortical regions of interest, voxels within the basal forebrain and thalamus were masked out of analyses using the SPM12 default settings. To examine arousal-related activity in these regions, the SNR setting (i.e. mean activity divided by the standard deviation of activity in each voxel) was changed from the default value of 0.8 to 0.2 and the subject-level SPM models were re-run. Small volume correction was then applied using anatomical masks of the basal forebrain (Zaborszky et al., 2008) and thalamus (Johansen-Berg et al., 2005). To ensure that neighboring CSF voxels were not included, these masks were modified to exclude any voxels that overlapped with the automated anatomical labeling atlas ventricle map. The small volume correction analysis was thresholded at a voxel-wise p-value of $p < 0.001$. An exploratory analysis of brainstem arousal-related activity was performed using a low threshold ($p < 0.05$, uncorrected). This analysis was performed to identify those brainstem nuclei that display arousal-related activity and to determine whether arousal-related activity was found within well-established sympathetic (Rostral Ventrolateral Medulla: RVLM, and Locus Coeruleus: LC) nuclei.

2.5.4. Follow-up examination of inter-individual associations between cardiac-BOLD and RTs—To determine whether the strength of arousal-related activity was associated with individual differences in RTs, follow-up voxel-wise analyses were done to examine associations between the strength of the cardiac-BOLD activity with mean RTs on correct trials for the two tasks. For these analyses, group-level brain-behavior associations were tested by doing voxel-wise regressions separately for the cardiac-BOLD and HB-evoked contrast images predicting mean RTs. The R^2 values were then obtained for every voxel in which positive cardiac-BOLD activity was related to mean RTs ($R^2 > 0.1$).

2.5.5. Follow-up examination of resting-state connectivity of the ventrolateral pulvinar (VLP)—Peak thalamic cardiac-BOLD and HB-evoked activity was found in the VLP for all three task conditions. To determine whether this region may be a key node in translating information from the ARAS to thalamocortical circuits, intrinsic resting-state connectivity of this region was examined. For this analysis, CompCor nuisance regression, band-pass filtering (0.1–0.01 Hz) and 6-mm FWHM spatial smoothing was performed. Fisher's Z-transformed full-brain connectivity maps were then created for a 4-mm sphere placed at the peak VLP coordinate identified in the cardiac-BOLD analysis for both tasks (MNI coordinate: $x = -24$, $y = -34$, $z = -2$). Significant connectivity was identified by performing a one-sample t-test in SPM12. Follow-up brain-behavior analyses were performed to examine whether the strength of intrinsic VLP connectivity was related to inter-individual differences in HR or RTs. Since the same 20 participants completed both the resting-state and OBT runs, behavioral RT data was taken from the OBT.

3. Results

3.1. Behavioral

In the MSIT, participants were faster ($t(19) = 12.35$, $p < 0.001$) and more accurate ($t(19) = 5.03$, $p < 0.001$) on congruent (mean RT = 619.48 (78.07) msec, mean accuracy = 0.98 (0.031)) than interference trials (mean RT = 881.10 (133.73) msec, mean accuracy = 0.91

(0.081)). In the OBT, participants were faster ($t(19) = 9.73$, $p < 0.001$) and more accurate ($t(19) = 4.33$, $p < 0.001$) on standard (mean RT = 409.74 (50.76) msec, mean accuracy = 0.97 (0.021)) than oddball trials (mean RT = 471.44 (52.87) msec, mean accuracy = 0.90 (0.079)).

3.1.1. Behavior-heart rate associations—Physiological HR measures were examined for MSIT, OBT, and rest blocks. Participants had shorter IBIs ($t(19) = 5.04$, $p < 0.001$) during the MSIT (mean (SD) = 0.84 (0.12)) than during rest (mean (SD) = 0.87 (0.11)), indicating faster HR during task performance. Participants also had shorter IBIs ($t(19) = 4.55$, $p < 0.001$) during the OBT (mean (SD) = 0.83 (0.10)) than during rest (mean (SD) = 0.87(0.11)). Mean IBI did not differ between the MSIT and OBT ($t(19) = 0.51$, $p = 0.68$).

To examine the influence of task design on HR for each task, linear mixed models tested the effects of task condition and sHB during correct trials. For both tasks, there were no effects of task condition on HR; however, there were highly robust effects of sHB (Tables S1 and S2). This latter effect was driven by slower HR for the concurrent HB than for HBs occurring before or after the stimulus (Fig. 2).

For both the MSIT and OBT, HR was strongly associated with individual differences in task performance. To ensure that HR and RT measures were comparable, mean HR was computed for the concurrent HB of correct trials. For the MSIT, mean HR was associated with mean MSIT RTs ($r = -0.58$, $p = 0.0075$), such that participants with slower HR tended to have faster RTs (Fig. 3). Likewise for the OBT, participants with slower HR tended to have faster RTs ($r = -0.50$, $p = 0.025$).

To examine within-subject cardiac-performance relationships, linear mixed models examined the categorical effects of condition and rHB in addition to the continuous effects of cardiac metrics (concurrent HR or HSI) on RTs. It was found that after categorizing the trials according to condition and rHB, robust intra-subject relationships between cardiac metrics and RTs existed. The results are reported in Tables S3–S6. While there was an intra-subject RT-HR relationship for the OBT, the intra-subject RT-HSI relationship was much stronger for both tasks. This latter relationship was found in all subjects and generally occurred across both tasks and within each task condition (see Fig. 4 for RT-HSI associations in two exemplar participants).

3.2. fMRI

3.2.1. Cortical arousal-related activity—For both tasks and for rest, activity across a broad distributed set of cortical regions was positively associated with the cardiac-BOLD regressor (Fig. 5). For the MSIT, this autonomic arousal-related activity was found though out an extensive set of visual, attention, and cognitive control regions (Fig. 5, top panel). This cardiac-BOLD activity occurred mainly within visual, dorsal attention, and frontoparietal regions. For the OBT, arousal-related activity was found in a set of attention network and frontoparietal cortical regions that was, for the most part, distinct from those found for the MSIT. This activity was mainly confined to the frontoparietal network, but unlike the MSIT, arousal-related activity extended into inferior frontal and dorsal insula

regions. In addition, while arousal-related activity in the MSIT was most robust in ventral visual stream regions (i.e. occipital and inferior temporal cortices). Arousal-related activity in the OBT was not significant in these regions. During rest, arousal-related activity was primarily confined within these ventral visual stream regions, and was much less extensive than that of either task.

In addition to examining arousal-related activity associated with the cardiac-BOLD regressor, HB-evoked activity that was associated with the unmodulated cardiac regressor was also examined. Negative HB-evoked activity was found across a set of regions that are commonly engaged by autonomic processing and are considered to form the AN, including MPFC, dorsal ACC, SMC, and the anterior and posterior insula (Critchley, 2009; Shoemaker et al., 2015). This HB-evoked suppression was found across all three task conditions (although dACC and SMC negative activity was weaker in the OBT than during MSIT or rest). In addition, positive HB-evoked activity was found in occipital and posterior parietal cortices for all three conditions. This latter activity was weaker than the negatively-associated HB-evoked activity and did not survive multiple-comparisons correction. It is notable, nonetheless, since it occurred within some of the same regions showing arousal-related activity.

Follow-up analyses examined the overlap between cardiac-BOLD activity and task-evoked activity by excluding the cardiac-BOLD regressors from the subject-level GLMs. Figs. S4 and S5 show that while the localization of task-evoked activity was not affected by the inclusion of cardiac-BOLD regressors, activity was much more robust and extensive with them included in the models.

Additional follow-up analyses examined the effect of CompCor physiological nuisance regressors on both cardiac-BOLD activity and task-evoked activity. Figs. S6 and S7 show that the localization of both cardiac-BOLD and task evoked activity was similar with and without CompCor physiological nuisance regressors; however, both cardiac-BOLD and task-evoked activity was more extensive and robust with the physiological nuisance regressors included in the subject-level models.

Recent studies have found that negative BOLD signals in periventricular regions are attributable to respiratory changes and are strongly related to the Global Signal (Bianciardi et al., 2011; Bright et al., 2014). To further investigate the potential relationship between physiological respiratory changes and cardiac-BOLD activity, we examined the relationship of the Global Signal Regressor with the cardiac regressors and with the CompCor physiological nuisance regressors. We found that the Global Signal Regressor was much more closely related to the physiological nuisance regressors than to the cardiac regressors (Fig. S8), suggesting that cardiac-BOLD activity does not merely reflect vascular changes associated with respiration.

3.2.2. Subcortical arousal-related activity—While no significant basal forebrain activity was found, both positive cardiac-BOLD and negative cardiac-BOLD activity occurred within the thalamus. Fig. 6 displays the thalamic voxels with significant arousal-related thalamic activity, at a voxel-level threshold of $p < 0.001$ and a set-level threshold of p

< 0.002. This activity was mostly confined to the pulvinar nucleus across all three tasks. Notably, arousal-related activity in the VLP was positively associated with the cardiac-BOLD regressor for both tasks. This region plays a causal role in coordinating cortical activity in the service of visual attention and is critical for task performance (Purushothaman et al., 2012; Zhou et al., 2016). Dropping the threshold to $p < 0.01$ revealed more extensive arousal-related activity in the VLP as well as in the medial dorsal and ventral lateral nuclei for both tasks. No positive arousal-related activity was found at either threshold during the rest condition. On the other hand, negative arousal-related activity was found in a separate dorsal pulvinar region in all three task conditions, and was in fact, strongest in the rest condition. During rest, this negative arousal-related activity occurred in the pulvinar and extended into the dorsal lateral, anterior, and midline thalamic nuclei.

Examination of HB-evoked thalamic activity (i.e. activity associated with the unmodulated cardiac regressor) revealed that positive HB-evoked VLP activity occurred during all three task conditions and localized to a similar region as the arousal-related VLP identified during both tasks. To determine whether the VLP is critical for translating arousal activity from brainstem circuits to the cortex, full-brain resting-state VLP connectivity was examined for the peak VLP coordinate showing arousal-related activity in both tasks. There was striking spatial correspondence between HB-evoked activity in all three conditions and resting-state VLP connectivity (Fig. S9), consistent with the interpretation that the thalamus is a critical node for ascending HB-evoked cortical activity.

To further examine the subcortical aspects of arousal-related activity, an exploratory analysis of the brainstem revealed positive activity in an extensive region of the dorsal pons for both the MSIT and OBT (Fig. 7). This region falls within the pontine reticular formation, part of the ARAS (Edlow et al., 2012; Yeo et al., 2013), consistent with the interpretation that arousal-related cortical activity originates in ascending brainstem pathways. A small, weaker activation was also found in the rest condition in a slightly inferior pontine region. In addition, negative arousal-related brainstem activity occurred in the arcuate nucleus of the medulla during all three conditions. During the rest condition, negative arousal-related activity in the medulla was more robust and extended into the RVLM. Since the latter is a region with a well-known role in baroreceptor-mediated arousal-related activity, we also examined whether subthreshold activity in this region was found during either task. Weak, subthreshold negative arousal-related activity was found for both tasks at RVLM coordinates previously identified as related to spontaneous fluctuations in muscle sympathetic nerve activity (Kobuch et al., 2018; Macefield and Henderson, 2019). The RVLM plays an important role in cerebral autoregulation by initiating vasoconstriction upon baroreceptor unloading (Kobuch et al., 2018; Macefield and Henderson, 2019) and therefore, a potential vascular mechanism could be responsible for general increases in cardiac-BOLD activity. However, given the very weak RVLM arousal-related activity found during both tasks, this mechanism is unlikely to account for the current findings. Arousal-related activity in the LC was also examined to further interrogate brainstem nuclei involved in sympathetic arousal. Examining activity in peak coordinates from a previous study focusing on LC circuitry (Song et al., 2017), subthreshold negative arousal-related activity was found for all three task conditions. Further, given that LC localization is variable across subjects, we examined activity across a more extensive set of LC coordinates (Keren et al., 2015) and found that in

all cases, arousal-related activity was subthreshold and tended to be negatively associated with cardiac-BOLD activity.

3.2.3. Associations between arousal-related activity and performance—To determine whether arousal-related activity was associated with individual differences in performance, associations between the first-level cardiac regressor contrasts and RTs were performed for those voxels showing significant arousal-related activity in each task. Fig. S10 shows that while brain-behavior associations were found for both unmodulated cardiac and cardiac-BOLD regressors of the first-level GLMs, associations were more extensive with the unmodulated cardiac contrasts. This suggests that subject's with faster RTs have greater HB-evoked activity overall.

3.2.4. Associations between intrinsic resting-state VLP connectivity and behavior—Since thalamic oscillatory activity is likely responsible for propagating arousal-related activity to cortex, we examined whether intrinsic VLP connectivity is related to inter-individual differences in autonomic function and behavior (i.e. HR and RTs on the OBT). Due to the relatively small sample size, these analyses were thresholded at a voxel-level p-value<0.05 and a cluster-level p-value<0.001. We found a broad set of cortical regions that were associated with both HR and RTs (Fig. S11).

4. Discussion

The current study identified widespread cortical and subcortical fluctuations in activity associated with autonomic arousal. The amplitude of activation increased with slower HR, suggesting that neuronal activity in these regions is dependent on the degree of momentary parasympathetic arousal. Cortical arousal-related activity was task-specific. During rest, arousal-related activity was restricted to visual regions; while during the MSIT, activity occurred not only in visual regions, but also across a distributed set of dorsal attention network regions (Corbetta et al., 2002; Fox et al., 2006). During the OBT, arousal-related activity occurred mainly within frontoparietal cortex (Vincent et al., 2008). Accompanying this arousal-related cortical activity was arousal-related activity of the thalamus and dorsal pons during both tasks. Thalamic activity was strongest in the pulvinar nucleus, a region with widespread ascending cortical projections that plays a well-established role in coordinating activity across cortical regions to facilitate visual attention (Jaramillo et al., 2019; Saalmann et al., 2012; Zhou et al., 2016). Arousal activity in the dorsal pons fell within the pontine reticular formation, which forms part of the ARAS (Edlow et al., 2012; Jang and Kwon, 2015b; Moruzzi and Magoun, 1949; Yeo et al., 2013). Therefore, the subcortical cardiac-BOLD findings are consistent with the interpretation that arousal-related activity is propagated through ascending autonomic arousal circuits. Brainstem nuclei that are commonly associated with sympathetic arousal (i.e. RVLM and LC) showed weakly negative arousal-related activity providing further support for a parasympathetic mechanism.

Bidirectional influences between HR and task performance were found in both tasks. On average, HR increased during performance of both tasks compared to rest, consistent with the view that cognitive tasks are cardiovascular challenges (Sheu et al., 2012). On-going fluctuations in HR during task performance slowed at stimulus presentation, but were not

impacted by the current trial task condition (Fig. 2). Fluctuations in HR were, on the other hand, related to on-going behavior; however, task performance was more strongly related to HSI (a metric that is dependent on both the concurrent HR and the stimulus timing with respect to the HB) than to HR itself (Fig. 4). Individual differences in processing speed were robustly associated with mean HR (accounting for 33% of the variance in RTs in the MSIT and 25% in the OBT: Fig. 3). The findings suggest that fluctuations in parasympathetic arousal activate distributed thalamocortical networks which facilitate cognitive processing when cardiac timing is optimized with respect to the task.

4.1. Autonomic arousal-related activity

The current study found that cortical arousal tended to occur when HR was slower, suggesting that this HR-related brain activity is mediated by the parasympathetic, rather than the sympathetic, nervous system. Distinct and opposing parasympathetic and sympathetic arousal-related ascending brainstem pathways exist, which are directly influenced by cardiac baroreceptor activity (Silvani et al., 2015). The primary brainstem nucleus affecting the sympathetic pathway is RVLM and activity in this region is tightly coupled with fluctuations in Muscle Sympathetic Nerve Activity (MSNA), which is suppressed on each HB by parasympathetic baroreceptor firing (Macefield and Henderson, 2019; Taylor et al., 2016). MSNA-related activity has also previously been found across a number of AN regions including the anterior and posterior insula, amygdala, cingulate cortex, MPFC, and SMC (Kobuch et al., 2018; Macefield and Henderson, 2019; Taylor et al., 2016). These AN regions are commonly associated with evoked sympathetic responses to a number of cognitive, nociceptive, and/or cardiovascular challenges (Beissner et al., 2013; Critchley, 2009; Maihofner et al., 2011; Patterson et al., 2002; Shoemaker et al., 2015).

While the current study did identify arousal-related activity in the anterior insula for both tasks, most AN regions were not strongly affected by HR. Instead, strong negative associations between activity in AN regions and the unmodulated cardiac regressor existed. This HB-evoked suppression of AN activity may reflect the suppression of descending autonomic pathways. HB-evoked activity has been found in numerous electroencephalography and electrocorticography studies (Kern et al., 2013; Lechinger et al., 2015); and, similar to HR-related activity, this activity may result from baroreceptor firing occurring upon each HB.

During both tasks and rest, there was not only strong HB-evoked suppression of activity across AN regions, but also opposing HB-evoked activation in visual processing regions (i.e. occipital and posterior parietal cortices). Like the arousal-related activity associated with HR slowing, this latter HB-evoked activation may be due to baroreceptor-mediated ascending activity originating in autonomic brainstem nuclei (Silvani et al., 2015). To determine whether the cardiac-BOLD activity could be propagated through ascending thalamocortical circuits, we examined resting-state connectivity of the VLP and found striking spatial correspondence between intrinsic VLP connectivity and HB-evoked activity during all three task conditions (Fig. S9). The strength of intrinsic VLP connectivity was associated with inter-individual differences in both HR and RTs across subcortical and cortical regions (Fig.

S11). Therefore, the findings support the role of ascending thalamocortical circuits in autonomic cortical arousal.

Recent studies have found fluctuations in widespread activation related to momentary fluctuations in alertness during rest. Periods of globally-increased activity across widespread cortical regions tend to co-occur with periods of heightened alertness (Falahpour et al., 2018; Liu et al., 2018; Turchi et al., 2018). Such alertness-related activity has also been attributed to activity in ARAS regions which project broadly to cortex (Edlow et al., 2012; Jang and Kwon, 2015a; Yeo et al., 2013). Other studies have found reduced cortical connectivity during states of low alertness such as sleep deprivation (Wang et al., 2016) and a growing number of studies are examining the overlap between ascending pathways supporting wakefulness and those supporting autonomic arousal (Satpute et al., 2019). The current findings suggest that autonomic arousal-related activation supports, not just alertness, but also visual attention during task performance. This interpretation is supported both by the presence of arousal-related activity across visual/attention networks and by the relationship between cardiac timing and intra-subject improvements in behavioral performance. Participants with slower HR tended to respond faster during both tasks and robust intra-subject cardiac-RT relationships were found. Intra-subject performance, however, was more strongly related to the HSI than HR itself. HSI is a measure of stimulus timing with respect to the prior HB and is highly dependent on HR (trials with longer HR also tend to have longer HSI). Trial-level performance improvements therefore depend, not only on increased arousal associated with slower HR, but also on optimal stimulus timing. Performance may benefit when perceptual processing of task events is facilitated by momentary increases in parasympathetic arousal of visual and attention networks.

4.2. Autonomic arousal and physiological noise

The current findings suggest that cardiac-related fMRI activity reflects, at least in part, fluctuating cognitive states. While, traditionally, physiological metrics have been used to de-noise fMRI data, we find low-frequency cardiac-related fMRI signal that can be attributable to neuronal activity. This signal resembles the BOLD response, is found across an extensive set of cortical and subcortical grey matter regions, and occurs within cardiac ascending arousal circuits. To further distinguish this arousal-related activity from physiological noise, our primary analytic models included both cardiac-BOLD and physiological noise regressors (identified based on signal variation within white matter and CSF voxels, using the CompCor method (Behzadi et al., 2007; Muschelli et al., 2014)). The use of these noise regressors did not reduce arousal-related activity. Instead, inclusion of physiological noise regressors, improved detection of autonomic arousal-related activation (Figs. S6 and S7). Further, inclusion of both the cardiac regressors and physiological noise regressors improved model fit and the detection of task-evoked effects compared to the use of cardiac regressors only, physiological noise regressors only, or neither set of regressors (Figs. S4–S7). The results support the interpretation that the cardiac-BOLD signal is distinct from task-evoked activity as well as the higher-frequency cardiac and respiratory pulsatility that is commonly removed during fMRI de-noising.

Identification of robust cardiac-BOLD activity in subcortical ascending arousal circuitry, such as the thalamus and dorsal pons (Silvani et al., 2015), provides further support that the arousal-related activity found in the current study reflects neuronal activity rather than cardiovascular changes associated with fluctuations in HR. However, the presence of robust ventricular activation, which was negatively associated with both the cardiac-BOLD and unmodulated cardiac regressors in the current study, raises the possibility that there is a vascular contribution to cardiac-BOLD activity. Recent studies have attributed periventricular negative BOLD signals to increased flow in the periventricular vasculature and to accompanying decreased ventricular volume (Bianciardi et al., 2011; Bright et al., 2014; Ozbay et al., 2018). These effects reflect vascular changes associated with respiration and/or cerebral autoregulation (Bianciardi et al., 2011; Bright et al., 2014; Ozbay et al., 2018). Similar periventricular negative BOLD signal changes have also been found in task-evoked activity in response to a VisualMotor task fMRI paradigm (Bright et al., 2014), suggesting that such physiological vascular changes affect the periventricular BOLD response even in the absence of an explicit cardiovascular challenge.

Although this periventricular physiological signal was present in the current datasets, it is unlikely that the positive cardiac-BOLD activity is likewise attributable to global systemic changes in vasculature for a couple reasons. First, respiratory changes and photoplethysmograph amplitude, reflecting large-scale vascular changes, are both closely associated with the fMRI Global Signal (Bright et al., 2014; Ozbay et al., 2018); while the cardiac regressors in the current study show a much more modest relationship with the Global Signal Regressor (Fig. S8). Second, we have found that positive cardiac-BOLD activity is robust to the removal of low photoplethysmograph amplitude events (i.e. 3 consecutive HBs with amplitude in the bottom 15% for each run), which may reflect cerebral autoregulation (Ozbay et al., 2018)). Therefore, while there may be some physiological contribution to the cardiac-BOLD signal, there is evidence that positive arousal-related activity reflects neuronal activity originating in ascending arousal pathways.

4.3. Subcortical arousal-related activity

A growing body of research has examined the role of the thalamus, and the pulvinar nucleus in particular, in coordinating activity within and across cortical regions to promote sustained and/or selective attention. Thalamocortical loops generate oscillatory activity, which promotes communication between cortical networks and is critical for both consciousness and sleep/wake states (Crick, 1984; Ferrarelli and Tononi, 2011, 2017). The pulvinar nucleus is an associative thalamic region involved in amplifying cortical communication to promote attention to salient visual stimuli. This region contains several retinotopic maps providing its own crude visual representation, which primarily serves to boost activity within and between visual and attention network regions (Arcaro et al., 2015; Shipp, 2003). The pulvinar receives direct input from the brainstem ARAS and processing within corticopulvinocortical loops is strongly influenced by the Thalamic Reticular Nucleus (TRN), which is also a direct recipient of inputs from the brainstem ARAS (Crick, 1984; Ferrarelli and Tononi, 2011; Nakajima and Halassa, 2017; Saalmann et al., 2012). TRN activity has widespread effects, influencing all other thalamic nuclei through GABAergic inhibition. TRN neurons modulate visual attention through their inhibitory influence on corticopulvinocortical loops and are

commonly included as an integral part of corticopulvinocortical loop models (Jaramillo et al., 2019; Nakajima and Halassa, 2017). While the size and morphology of the TRN make it difficult to directly detect activity using fMRI, it is notable that this nucleus likely plays a highly influential role in cortical arousal through ascending autonomic circuits.

In the current study, the VLP showed positive parasympathetic arousal-related activity for both tasks, but not for rest. It did, however, show strong positive HB-evoked activity during all three task conditions, including robust activity during rest, consistent with the interpretation that this region is a critical node for propagating baroreceptor-mediated ascending autonomic arousal from the brainstem to cortex. The pattern of HB-evoked activity showed striking similarities to the resting-state functional connectivity map of the VLP (Fig. S9), with positive arousal-related activity occurring across occipital/posterior parietal cortex and negative arousal-related activity occurring in the MPFC. This spatial correspondence between intrinsic pulvinar connectivity and HB-evoked activity provides further support that cortical autonomic activity may be transmitted directly through this region. The thalamus, in general, plays a well-known role in propagating oscillatory activity through thalamocortical circuits to sustain states of wakefulness or attention (Chen et al., 2015; Halassa et al., 2014). Therefore, it is likely that the VLP, as well as the thalamic dorsomedial nucleus, which also showed arousal-related activity for both tasks, promotes arousal states by propagating baroreceptor-mediated ARAS activity onto cortical circuits.

Consistent with the interpretation that widespread cardiac-BOLD activity across cortical regions reflects ascending rather than descending circuits, we found arousal-related activity in the pontine reticular formation for both tasks. This region forms part of the ARAS (Edlow et al., 2012; Moruzzi and Magoun, 1949) and plays a role in both autonomic processing and wakefulness (Satpute et al., 2019). Further, this ARAS region has been implicated in attention (Kinomura et al., 1996). The dorsal pons is important for coordinating eye movements and processing within this region is directly involved in facilitating visual attention by coordinating autonomic, visual, and motoric information (Cohen and Komatsuzaki, 1972; Gandhi et al., 2008; Ter Horst et al., 1991). The pontine reticular formation may therefore provide an early site of integration across these modalities.

5. Conclusions

Parasympathetic arousal is associated with greater cortical activation as well as improved cognitive performance. Arousal-related activity occurred in an extensive set of distributed, task-specific cortical regions during two tasks and rest. Consistent with the interpretation that this arousal-related activity reflects autonomic arousal propagated through ascending circuits originating in the brainstem, arousal-related activity was found in the thalamus and dorsal pons. Peak thalamic arousal occurred in the pulvinar nucleus for all three conditions, suggesting that this region is important for propagating information from ARAS brainstem regions to the cortex. Although arousal-related activity occurred in ARAS circuits, the task-specific nature of the cortical arousal implies that this activity is modified by top-down contextual demands.

Strong associations were found between cardiac metrics and task performance. Individuals with slower HR (i.e. more parasympathetic arousal) had faster RTs. Examination of within-subject, trial-level cardiac-performance coupling revealed that RTs were dependent on the relative timing between cardiac and stimulus events. This suggests that parasympathetic arousal provides an additional source of trial-level variability in RTs that is separate from task-evoked RT-related activity (Barber et al., 2016, 2017; Prado and Weissman, 2011). Fluctuations in parasympathetic arousal may thereby promote attention when there is optimal overlap between arousal and task events. The findings suggest that autonomic arousal-related activity reflects a novel, yet important, component of cognitive processing and should be integrated into neurobiological models of cognition and mental health.

Supplementary Material

Refer to Web version on PubMed Central for supplementary material.

Acknowledgments

Supported by NIMH grant R01MH108654 to Dr. Malhotra.

References

Arcaro MJ, Pinsk MA, Kastner S, 2015 The anatomical and functional organization of the human visual pulvinar. J. Neurosci. 35, 9848–9871. [PubMed: 26156987]

Barber AD, Caffo BS, Pekar JJ, Mostofsky SH, 2017 Decoupling of reaction time-related default mode network activity with cognitive demand. Brain Imag. Behav. 11, 666–676.

Barber AD, Pekar JJ, Mostofsky SH, 2016 Reaction time-related activity reflecting periodic, task-specific cognitive control. Behav. Brain Res. 296, 100–108. [PubMed: 26318935]

Behzadi Y, Restom K, Liau J, Liu TT, 2007 A component based noise correction method (CompCor) for BOLD and perfusion based fMRI. Neuroimage 37, 90–101. [PubMed: 17560126]

Beissner F, Meissner K, Bar KJ, Napadow V, 2013 The autonomic brain: an activation likelihood estimation meta-analysis for central processing of autonomic function. J. Neurosci. 33, 10503–10511. [PubMed: 23785162]

Berntson GG, Sarter M, Cacioppo JT, 2003 Ascending visceral regulation of cortical affective information processing. Eur. J. Neurosci. 18, 2103–2109. [PubMed: 14622171]

Bianciardi M, Fukunaga M, van Gelderen P, de Zwart JA, Duyn JH, 2011 Negative BOLD-fMRI signals in large cerebral veins. J. Cereb. Blood Flow Metab. 31, 401–412. [PubMed: 20859295]

Bianciardi M, Fukunaga M, van Gelderen P, Horovitz SG, de Zwart JA, Shmueli K, Duyn JH, 2009 Sources of functional magnetic resonance imaging signal fluctuations in the human brain at rest: a 7 T study. Magn. Reson. Imaging 27, 1019–1029. [PubMed: 19375260]

Birren JE, Cardon PV Jr., Phillips SL, 1963 Reaction time as a function of the cardiac cycle in young adults. Science 140, 195–196.

Bright MG, Bianciardi M, de Zwart JA, Murphy K, Duyn JH, 2014 Early anticorrelated BOLD signal changes of physiologic origin. Neuroimage 87, 287–296. [PubMed: 24211818]

Burgess GC, Kandala S, Nolan D, Laumann TO, Power JD, Adeyemo B, Harms MP, Petersen SE, Barch DM, 2016 Evaluation of denoising strategies to address motion-correlated artifacts in resting-state functional magnetic resonance imaging data from the human connectome project. Brain Connect. 6, 669–680. [PubMed: 27571276]

Chang C, Cunningham JP, Glover GH, 2009 Influence of heart rate on the BOLD signal: the cardiac response function. Neuroimage 44, 857–869. [PubMed: 18951982]

Chang C, Glover GH, 2009 Effects of model-based physiological noise correction on default mode network anti-correlations and correlations. Neuroimage 47, 1448–1459. [PubMed: 19446646]

Chang C, Metzger CD, Glover GH, Duyn JH, Heinze HJ, Walter M, 2013 Association between heart rate variability and fluctuations in resting-state functional connectivity. Neuroimage 68, 93–104. [PubMed: 23246859]

Chee MW, Chuah LY, 2008 Functional neuroimaging insights into how sleep and sleep deprivation affect memory and cognition. Curr. Opin. Neurol. 21, 417–423. [PubMed: 18607201]

Chee MW, Tan JC, Zheng H, Parimal S, Weissman DH, Zagorodnov V, Dinges DF, 2008 Lapsing during sleep deprivation is associated with distributed changes in brain activation. J. Neurosci. 28, 5519–5528. [PubMed: 18495886]

Chen Z, Wimmer RD, Wilson MA, Halassa MM, 2015 Thalamic circuit mechanisms link sensory processing in sleep and attention. Front. Neural Circuits 9, 83. [PubMed: 26778969]

Ciric R, Wolf DH, Power JD, Roalf DR, Baum GL, Ruparel K, Shinohara RT, Elliott MA, Eickhoff SB, Davatzikos C, Gur RC, Gur RE, Bassett DS, Satterthwaite TD, 2017 Benchmarking of participant-level confound regression strategies for the control of motion artifact in studies of functional connectivity. Neuroimage 154, 174–187. [PubMed: 28302591]

Cohen B, Komatsuzaki A, 1972 Eye movements induced by stimulation of the pontine reticular formation: evidence for integration in oculomotor pathways. Exp. Neurol. 36, 101–117. [PubMed: 4558412]

Corbetta M, Kincade JM, Shulman GL, 2002 Neural systems for visual orienting and their relationships to spatial working memory. J. Cogn. Neurosci. 14, 508–523. [PubMed: 11970810]

Crick F, 1984 Function of the thalamic reticular complex: the searchlight hypothesis. Proc. Natl. Acad. Sci. U. S. A. 81, 4586–4590. [PubMed: 6589612]

Critchley HD, 2009 Psychophysiology of neural, cognitive and affective integration: fMRI and autonomic indicants. Int. J. Psychophysiol. 73, 88–94. [PubMed: 19414044]

Edlow BL, Takahashi E, Wu O, Benner T, Dai G, Bu L, Grant PE, Greer DM, Greenberg SM, Kinney HC, Folkerth RD, 2012 Neuroanatomic connectivity of the human ascending arousal system critical to consciousness and its disorders. J. Neuropathol. Exp. Neurol. 71, 531–546. [PubMed: 22592840]

Edwards L, Ring C, McIntyre D, Carroll D, Martin U, 2007 Psychomotor speed in hypertension: effects of reaction time components, stimulus modality, and phase of the cardiac cycle. Psychophysiology 44, 459–468. [PubMed: 17433098]

Eklund A, Knutsson H, Nichols TE, 2018 Cluster failure revisited: impact of first level design and physiological noise on cluster false positive rates. Hum. Brain Mapp.

Falahpour M, Chang C, Wong CW, Liu TT, 2018 Template-based prediction of vigilance fluctuations in resting-state fMRI. Neuroimage 174, 317–327. [PubMed: 29548849]

Fan J, Xu P, Van Dam NT, Eilam-Stock T, Gu X, Luo YJ, Hof PR, 2012 Spontaneous brain activity relates to autonomic arousal. J. Neurosci. 32, 11176–11186. [PubMed: 22895703]

Ferrarelli F, Tononi G, 2011 The thalamic reticular nucleus and schizophrenia. Schizophr. Bull. 37, 306–315. [PubMed: 21131368]

Ferrarelli F, Tononi G, 2017 Reduced sleep spindle activity point to a TRN-MD thalamus-PFC circuit dysfunction in schizophrenia. Schizophr. Res. 180, 36–43. [PubMed: 27269670]

Fox MD, Corbetta M, Snyder AZ, Vincent JL, Raichle ME, 2006 Spontaneous neuronal activity distinguishes human dorsal and ventral attention systems. Proc. Natl. Acad. Sci. U. S. A. 103, 10046–10051. [PubMed: 16788060]

Gandhi NJ, Barton EJ, Sparks DL, 2008 Coordination of eye and head components of movements evoked by stimulation of the paramedian pontine reticular formation. Exp. Brain Res. 189, 35–47. [PubMed: 18458891]

Garfinkel SN, Barrett AB, Minati L, Dolan RJ, Seth AK, Critchley HD, 2013 What the heart forgets: cardiac timing influences memory for words and is modulated by metacognition and interoceptive sensitivity. Psychophysiology 50, 505–512. [PubMed: 23521494]

Glover GH, Li TQ, Ress D, 2000 Image-based method for retrospective correction of physiological motion effects in fMRI: RETROICOR. Magn. Reson. Med. 44, 162–167. [PubMed: 10893535]

Halassa MM, Chen Z, Wimmer RD, Brunetti PM, Zhao S, Zikopoulos B, Wang F, Brown EN, Wilson MA, 2014 State-dependent architecture of thalamic reticular subnetworks. Cell 158, 808–821. [PubMed: 25126786]

Hansen AL, Johnsen BH, Thayer JF, 2003 Vagal influence on working memory and attention. Int. J. Psychophysiol. 48, 263–274. [PubMed: 12798986]

Jang SH, Kwon HG, 2015a The ascending reticular activating system from pontine reticular formation to the hypothalamus in the human brain: a diffusion tensor imaging study. Neurosci. Lett. 590, 58–61. [PubMed: 25641134]

Jang SH, Kwon HG, 2015b The direct pathway from the brainstem reticular formation to the cerebral cortex in the ascending reticular activating system: a diffusion tensor imaging study. Neurosci. Lett. 606, 200–203. [PubMed: 26363340]

Jaramillo J, Mejias JF, Wang XJ, 2019 Engagement of pulvino-cortical feedforward and feedback pathways in cognitive computations. Neuron 101, 321–336 e329. [PubMed: 30553546]

Johansen-Berg H, Behrens TE, Sillery E, Ciccarelli O, Thompson AJ, Smith SM, Matthews PM, 2005 Functional-anatomical validation and individual variation of diffusion tractography-based segmentation of the human thalamus. Cerebr. Cortex 15, 31–39.

Keren NI, Taheri S, Vazey EM, Morgan PS, Granholm AC, Aston-Jones GS, Eckert MA, 2015 Histologic validation of locus coeruleus MRI contrast in postmortem tissue. Neuroimage 113, 235–245. [PubMed: 25791783]

Kern M, Aertsen A, Schulze-Bonhage A, Ball T, 2013 Heart cycle-related effects on event-related potentials, spectral power changes, and connectivity patterns in the human ECoG. Neuroimage 81, 178–190. [PubMed: 23684883]

Kinomura S, Larsson J, Gulyas B, Roland PE, 1996 Activation by attention of the human reticular formation and thalamic intralaminar nuclei. Science 271, 512–515. [PubMed: 8560267]

Kobuch S, Macefield VG, Henderson LA, 2018 Resting regional brain activity and connectivity vary with resting blood pressure but not muscle sympathetic nerve activity in normotensive humans: an exploratory study. J. Cereb. Blood Flow Metab. 271678X18798442.

Lechinger J, Heib DP, Gruber W, Schabus M, Klimesch W, 2015 Heartbeat-related EEG amplitude and phase modulations from wakefulness to deep sleep: interactions with sleep spindles and slow oscillations. Psychophysiology 52, 1441–1450. [PubMed: 26268858]

Liu X, de Zwart JA, Scholvinck ML, Chang C, Ye FQ, Leopold DA, Duyn JH, 2018 Subcortical evidence for a contribution of arousal to fMRI studies of brain activity. Nat. Commun. 9, 395. [PubMed: 29374172]

Macefield VG, Henderson LA, 2019 Identification of the human sympathetic connectome involved in blood pressure regulation. Neuroimage 202, 116119. [PubMed: 31446130]

Maihofner C, Seifert F, Decol R, 2011 Activation of central sympathetic networks during innocuous and noxious somatosensory stimulation. Neuroimage 55, 216–224. [PubMed: 21126587]

McIntyre D, Ring C, Edwards L, Carroll D, 2008 Simple reaction time as a function of the phase of the cardiac cycle in young adults at risk for hypertension. Psychophysiology 45, 333–336. [PubMed: 17995912]

Moruzzi G, Magoun HW, 1949 Brain stem reticular formation and activation of the EEG. Electroencephalogr. Clin. Neurophysiol. 1, 455–473. [PubMed: 18421835]

Muschelli J, Nebel MB, Caffo BS, Barber AD, Pekar JJ, Mostofsky SH, 2014 Reduction of motion-related artifacts in resting state fMRI using aCompCor. Neuroimage 96, 22–35. [PubMed: 24657780]

Nakajima M, Halassa MM, 2017 Thalamic control of functional cortical connectivity. Curr. Opin. Neurobiol. 44, 127–131. [PubMed: 28486176]

Ozbay PS, Chang C, Picchioni D, Mandelkow H, Moehlman TM, Chappel-Farley MG, van Gelderen P, de Zwart JA, Duyn JH, 2018 Contribution of systemic vascular effects to fMRI activity in white matter. Neuroimage 176, 541–549. [PubMed: 29704614]

Patterson JC 2nd, Ungerleider LG, Bandettini PA, 2002 Task-independent functional brain activity correlation with skin conductance changes: an fMRI study. Neuroimage 17, 1797–1806. [PubMed: 12498753]

Porges SW, 1995 Cardiac vagal tone: a physiological index of stress. Neurosci. Biobehav. Rev. 19, 225–233. [PubMed: 7630578]

Porges SW, 2003 The Polyvagal Theory: phylogenetic contributions to social behavior. Physiol. Behav. 79, 503–513. [PubMed: 12954445]

Porges SW, 2007 The polyvagal perspective. Biol. Psychol. 74, 116–143. [PubMed: 17049418]

Porges SW, 2009 The polyvagal theory: new insights into adaptive reactions of the autonomic nervous system. Clevel. Clin. J. Med. 76 (Suppl. 2), S86–S90.

Porges SW, Doussard-Roosevelt JA, Maiti AK, 1994 Vagal tone and the physiological regulation of emotion. Monogr. Soc. Res. Child Dev. 59, 167–186. [PubMed: 7984159]

Power JD, Plitt M, Laumann TO, Martin A, 2017 Sources and implications of whole-brain fMRI signals in humans. Neuroimage 146, 609–625. [PubMed: 27751941]

Prado J, Weissman DH, 2011 Spatial attention influences trial-by-trial relationships between response time and functional connectivity in the visual cortex. Neuroimage 54, 465–473. [PubMed: 20736069]

Pramme L, Larra MF, Schachinger H, Frings C, 2016 Cardiac cycle time effects on selection efficiency in vision. Psychophysiology 53, 1702–1711. [PubMed: 27450530]

Purushothaman G, Marion R, Li K, Casagrande VA, 2012 Gating and control of primary visual cortex by pulvinar. Nat. Neurosci. 15, 905–912. [PubMed: 22561455]

Saalmann YB, Pinsk MA, Wang L, Li X, Kastner S, 2012 The pulvinar regulates information transmission between cortical areas based on attention demands. Science 337, 753–756. [PubMed: 22879517]

Saari MJ, Pappas BA, 1976 Cardiac cycle phase and movement and reaction times. Percept. Mot. Skills 42, 767–770. [PubMed: 1272724]

Sandman CA, 1984 Augmentation of the auditory event related potentials of the brain during diastole. Int. J. Psychophysiol. 2, 111–119. [PubMed: 6542913]

Saper CB, 2002 The central autonomic nervous system: conscious visceral perception and autonomic pattern generation. Annu. Rev. Neurosci. 25, 433–469. [PubMed: 12052916]

Satpute AB, Kragel PA, Barrett LF, Wager TD, Bianciardi M, 2019 Deconstructing arousal into wakeful, autonomic and affective varieties. Neurosci. Lett. 693, 19–28. [PubMed: 29378297]

Schmitt LI, Wimmer RD, Nakajima M, Happ M, Mofakham S, Halassa MM, 2017 Thalamic amplification of cortical connectivity sustains attentional control. Nature 545, 219–223. [PubMed: 28467827]

Sheu LK, Jennings JR, Gianaros PJ, 2012 Test-retest reliability of an fMRI paradigm for studies of cardiovascular reactivity. Psychophysiology 49, 873–884. [PubMed: 22594784]

Shipp S, 2003 The functional logic of cortico-pulvinar connections. Philos. Trans. R. Soc. Lond. B Biol. Sci. 358, 1605–1624. [PubMed: 14561322]

Shmueli K, van Gelderen P, de Zwart JA, Horovitz SG, Fukunaga M, Jansma JM, Duyn JH, 2007 Low-frequency fluctuations in the cardiac rate as a source of variance in the resting-state fMRI BOLD signal. Neuroimage 38, 306–320. [PubMed: 17869543]

Shoemaker JK, Norton KN, Baker J, Luchyshyn T, 2015 Forebrain organization for autonomic cardiovascular control. Auton. Neurosci. 188, 5–9. [PubMed: 25458433]

Silvani A, Calandra-Buonaura G, Benarroch EE, Dampney RA, Cortelli P, 2015 Bidirectional interactions between the baroreceptor reflex and arousal: an update. Sleep Med. 16, 210–216. [PubMed: 25616389]

Song AH, Kucyi A, Napadow V, Brown EN, Loggia ML, Akeju O, 2017 Pharmacological modulation of noradrenergic arousal circuitry disrupts functional connectivity of the locus ceruleus in humans. J. Neurosci. 37, 6938–6945. [PubMed: 28626012]

Suess PE, Porges SW, Plude DJ, 1994 Cardiac vagal tone and sustained attention in school-age children. Psychophysiology 31, 17–22. [PubMed: 8146250]

Taylor KS, Kucyi A, Millar PJ, Murai H, Kimmerly DS, Morris BL, Bradley TD, Floras JS, 2016 Association between resting-state brain functional connectivity and muscle sympathetic burst incidence. J. Neurophysiol. 115, 662–673. [PubMed: 26538607]

Ter Horst GJ, Copray JC, Liem RS, Van Willigen JD, 1991 Projections from the rostral parvocellular reticular formation to pontine and medullary nuclei in the rat: involvement in autonomic regulation and orofacial motor control. Neuroscience 40, 735–758. [PubMed: 2062440]

Thayer JF, Hansen AL, Saus-Rose E, Johnsen BH, 2009 Heart rate variability, prefrontal neural function, and cognitive performance: the neurovisceral integration perspective on self-regulation, adaptation, and health. Ann. Behav. Med 37, 141–153. [PubMed: 19424767]

Thayer JF, Siegle GJ, 2002 Neurovisceral integration in cardiac and emotional regulation. IEEE Eng. Med. Biol. Mag. 21, 24–29. [PubMed: 12222113]

Thayer JF, Yamamoto SS, Brosschot JF, 2010 The relationship of autonomic imbalance, heart rate variability and cardiovascular disease risk factors. Int. J. Cardiol. 141, 122–131. [PubMed: 19910061]

Turchi J, Chang C, Ye FQ, Russ BE, Yu DK, Cortes CR, Monosov IE, Duyn JH, Leopold DA, 2018 The basal forebrain regulates global resting-state fMRI fluctuations. Neuron 97, 940–952 e944. [PubMed: 29398365]

van der Molen MW, Somsen RJ, Orlebeke JF, 1983 Phasic heart rate responses and cardiac cycle time in auditory choice reaction time. Biol. Psychol. 16, 255–271. [PubMed: 6615957]

Van Essen DC, Smith SM, Barch DM, Behrens TE, Yacoub E, Ugurbil K, Consortium WU-MH, 2013 The Wu-Minn human connectome project: an overview. Neuroimage 80, 62–79. [PubMed: 23684880]

Vincent JL, Kahn I, Snyder AZ, Raichle ME, Buckner RL, 2008 Evidence for a frontoparietal control system revealed by intrinsic functional connectivity. J. Neurophysiol. 100, 3328–3342. [PubMed: 18799601]

Wang C, Ong JL, Patanaik A, Zhou J, Chee MW, 2016 Spontaneous eyelid closures link vigilance fluctuation with fMRI dynamic connectivity states. Proc. Natl. Acad. Sci. U. S. A. 113, 9653–9658. [PubMed: 27512040]

Worsley KJ, Cao J, Paus T, Petrides M, Evans AC, 1998 Applications of random field theory to functional connectivity. Hum. Brain Mapp. 6, 364–367. [PubMed: 9788073]

Worsley KJ, Taylor JE, Tomaiuolo F, Lerch J, 2004 Unified univariate and multivariate random field theory. Neuroimage 23 (Suppl. 1), S189–S195. [PubMed: 15501088]

Yeo SS, Chang PH, Jang SH, 2013 The ascending reticular activating system from pontine reticular formation to the thalamus in the human brain. Front. Hum. Neurosci. 7, 416. [PubMed: 23898258]

Zaborszky L, Hoemke L, Mohlberg H, Schleicher A, Amunts K, Zilles K, 2008 Stereotaxic probabilistic maps of the magnocellular cell groups in human basal forebrain. Neuroimage 42, 1127–1141. [PubMed: 18585468]

Zhou H, Schafer RJ, Desimone R, 2016 Pulvinar-cortex interactions in vision and attention. Neuron 89, 209–220. [PubMed: 26748092]

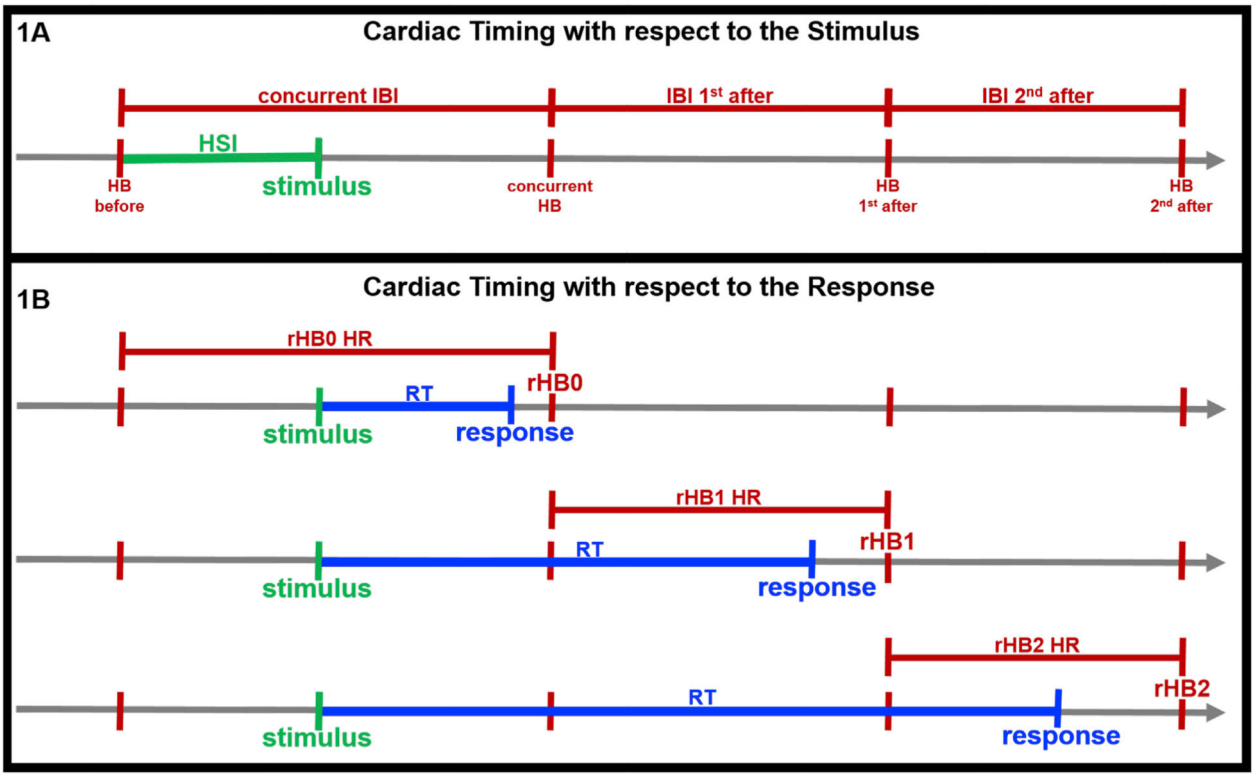

Fig. 1.

Cardiac timing with respect to a single trial. Heart Rate (HR) in the current study is represented by the Inter-Beat Interval. **1A. Cardiac timing with respect to the Stimulus.** The Heartbeat (HB)-Stimulus Interval (HSI) is the time from the HB just before the stimulus until the stimulus onset. The stimulus HB (sHB) is categorized into the HB occurring before, the HB concurrent with, the first HB after, or the second HB after the stimulus. **1B. Cardiac timing with respect to the Response.** Response HB (rHB) is categorized based on the number of post-stimulus HBs in which the response occurred (rHB0, rHB1, rHB2).

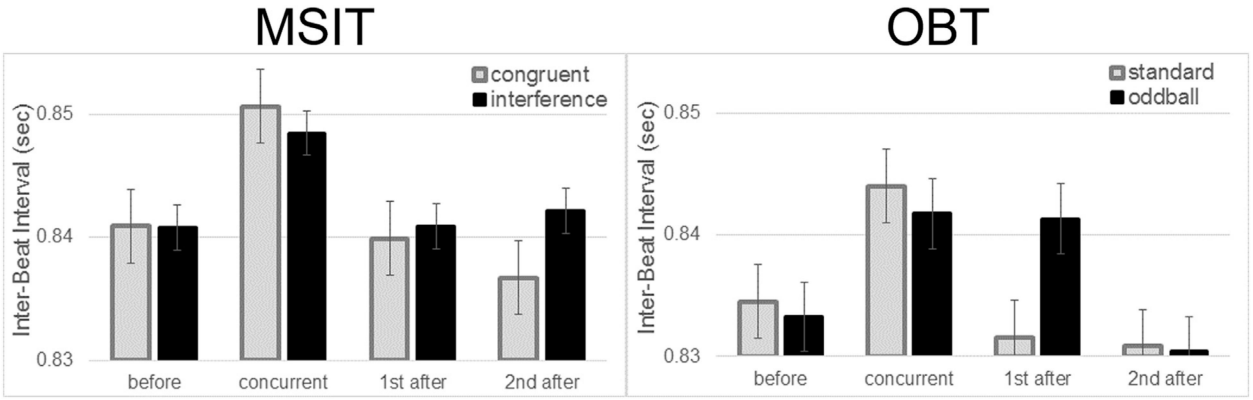

Fig. 2.

Mean Heart Rate (i.e. Inter-Beat Interval) for correct trials in the Multi-Source Interference Task (MSIT) and the Oddball Task (OBT). Heartbeats (HBs) were categorized by condition and by stimulus HB (sHB: one HB before, the HB concurrent with, the first HB after, or the second HB after the stimulus).

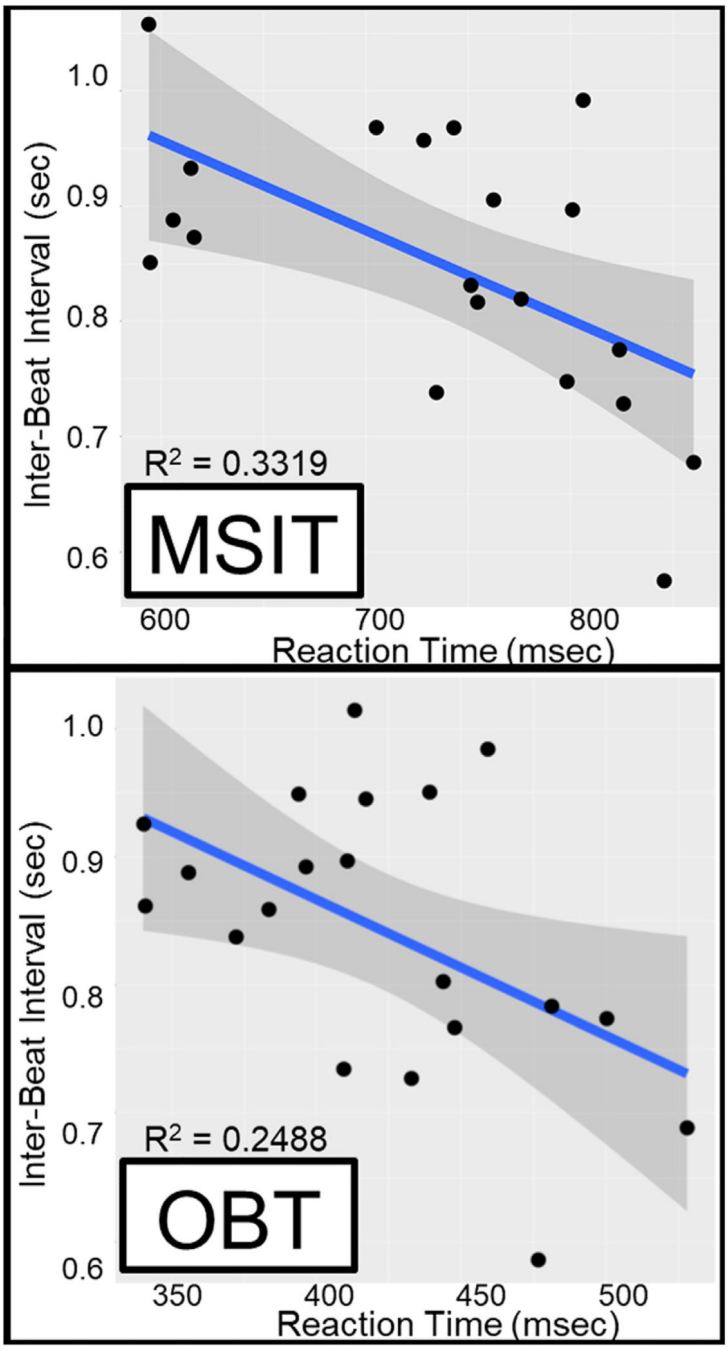

Fig. 3.

Inter-individual associations between Heart Rate (i.e. Inter-Beat Interval) and Reaction Time for the Multi-Source Interference Task (MSIT) and the Oddball Task (OBT). In both tasks, participants with slower Heart Rate tended to have faster processing speed.

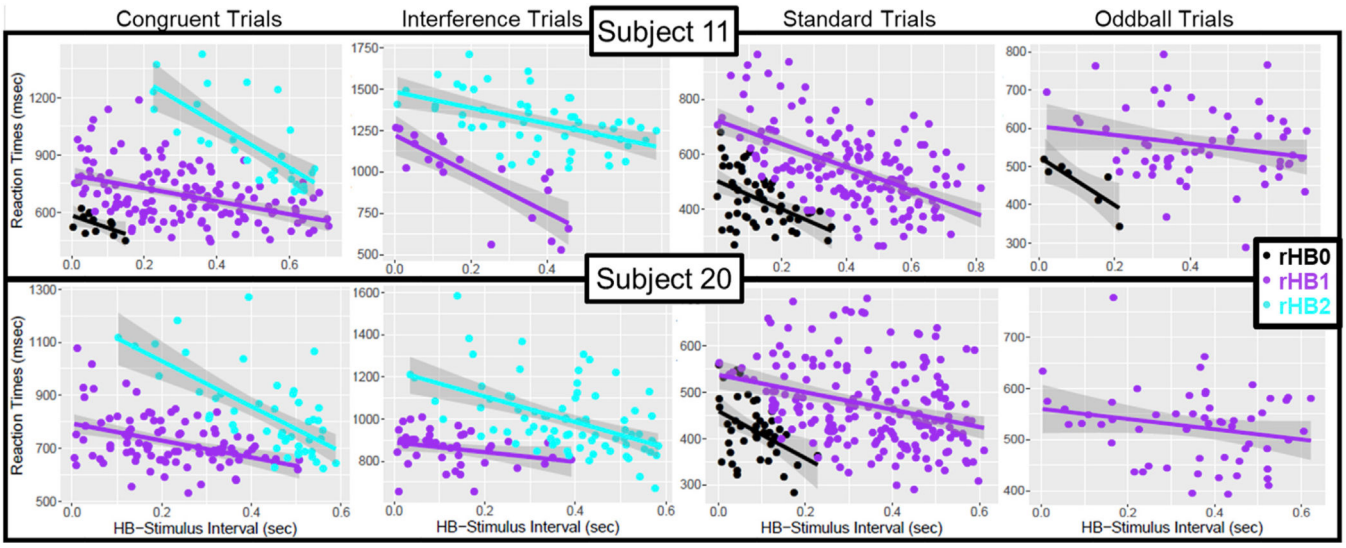

Fig. 4.

The intra-subject relationship between Reaction Times and Heartbeat (HB)-Stimulus Interval as a function of response HB (rHB) for two subjects. rHB0 are those trials in which the stimulus and response occurred within the same HB, rHB1 are those trials in which the response occurred one HB after the stimulus, and rHB2 are those trials in which the response occurred two HBs after the stimulus. Each column represents a different task condition: Congruent and Interference trials from the Multi-Source Interference Task (MSIT) and Standard and Oddball trials from the Oddball Task (OBT).

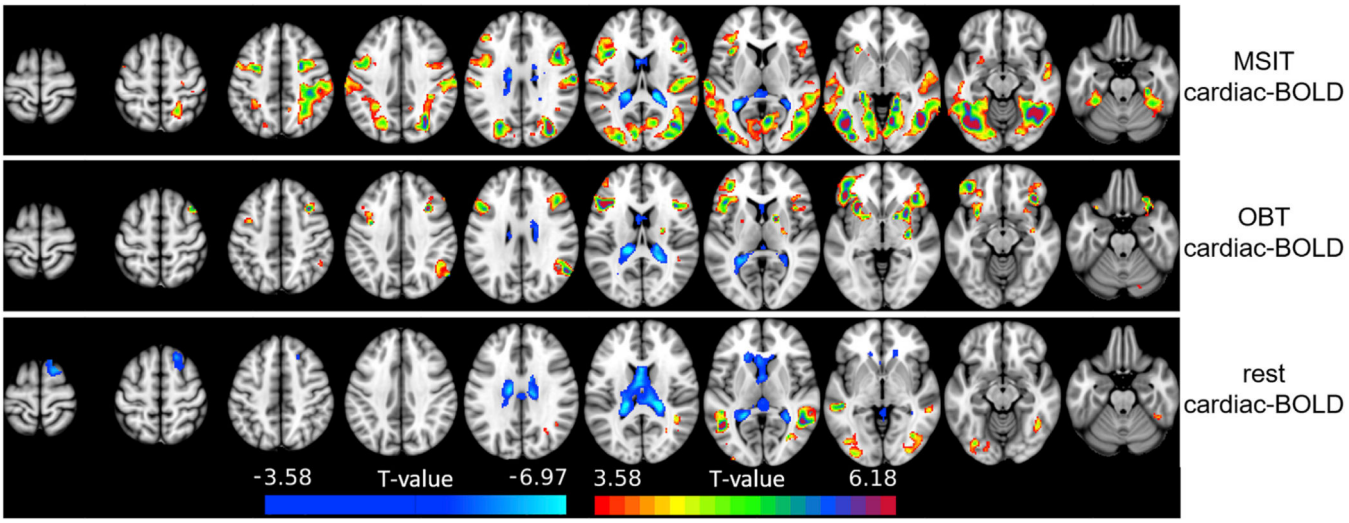

Fig. 5.

Arousal-related (i.e. cardiac-BOLD) activity for the three task conditions, thresholded at a voxel-level and cluster-level threshold of $p < 0.001$. Positive arousal-related activity reflected greater BOLD activity when Heart Rate (HR) was slower. Negative arousal-related activity reflected greater BOLD activity when HR was faster.

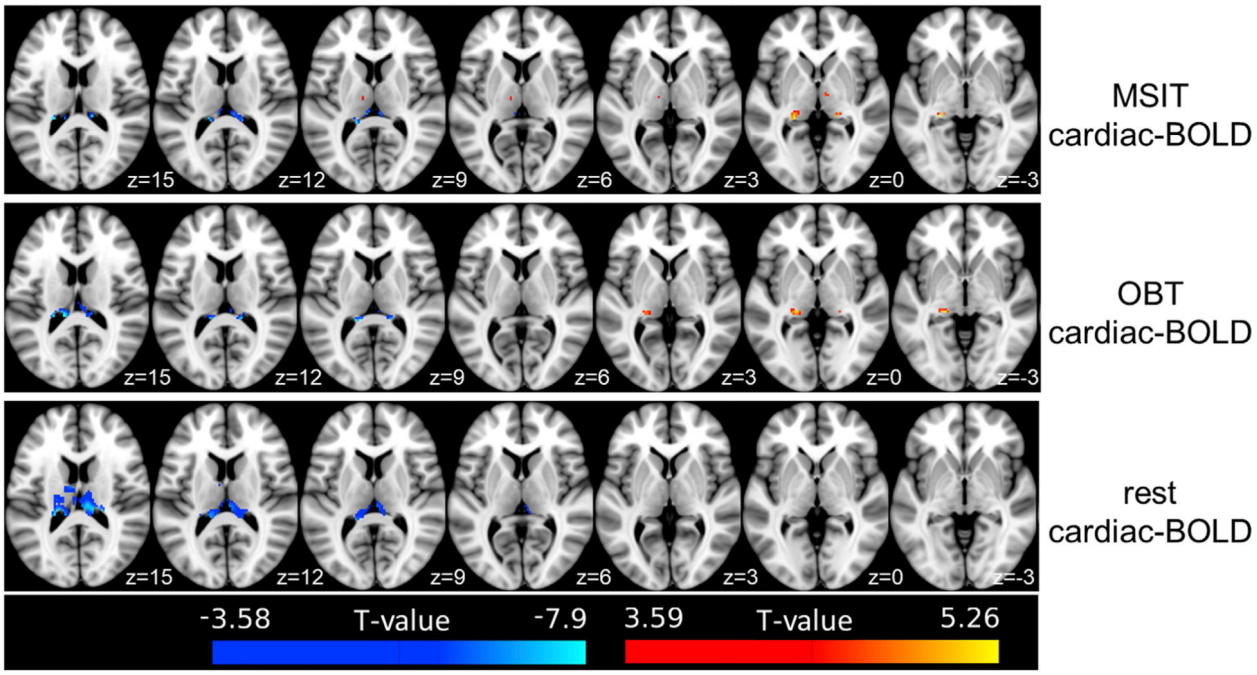

Fig. 6.

Thalamic arousal-related (i.e. cardiac-BOLD) activity for the three task conditions. Activity was thresholded at a voxel-level $p < 0.001$ and small-volume corrected at a set-level of $p < 0.002$. Positive arousal-related activity was found within the ventrolateral pulvinar for both the Multi-Source Interference Task (MSIT) and Oddball Task (OBT). Negative arousal-related activity was found within the posterior dorsal pulvinar for all three task conditions, but was most extensive during rest.

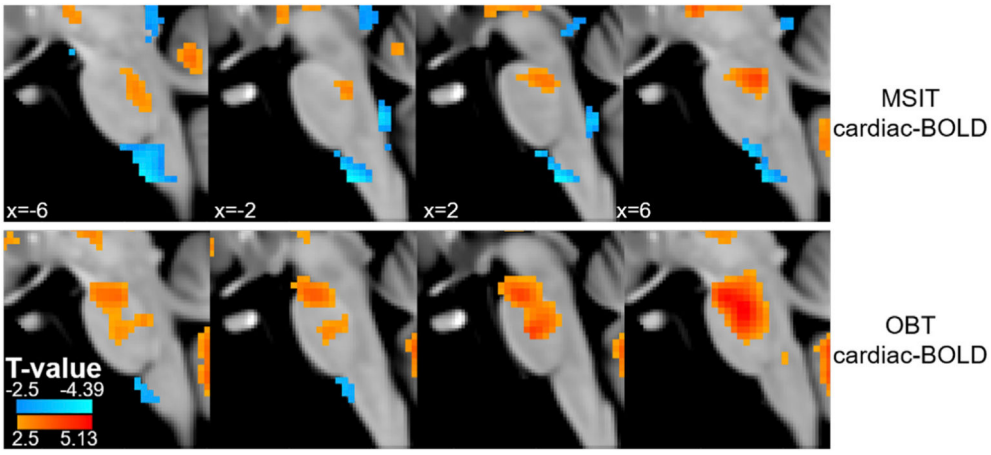

Fig. 7.

Brainstem arousal-related activity in the Multi-Source Interference Task (MSIT) and the Oddball Task (OBT).